Numerical Analysis of Natural Convection in a Concentric Trapezoidal Enclosure Filled with a Porous Medium

Article *in* International Journal of Engineering Research in Africa · July 2022

DOI: 10.4028/p-jza9vq

International Journal of Engineering Research in Africa
ISSN: 1663-4144, Vol. 61, pp 129-150
doi:10.4028/p-jza9vq

Submitted: 2021-12-17
Revised: 2022-06-13
Accepted: 2022-06-16
Online: 2022-07-25

Numerical Analysis of Natural Convection in a Concentric Trapezoidal Enclosure Filled with a Porous Medium

Olalekan Adebayo Olayemi*[1,2a], Muhammed Isiaka[1a], Khaled Al-Farhany[3b], Mohammed Azeez Alomari[3c], Muneer A. Ismael[4d], Sunday Olayinka Oyedepo[5e]

[1]Department of Aeronautics and Astronautics, Faculty of Engineering and Technology, Kwara State University, Malete, Kwara State, Nigeria.

[2]School of Engineering, Cranfield University, Cranfield, United Kingdom.

[3]Department of Mechanical Engineering, University of Al-Qadisiyah, Al-Qadisiyah, Iraq.

[4]Mechanical Engineering Department, Engineering College, University of Basrah, Basrah, Iraq.

[5]Department Mechanical Engineering, Covenant University, Ota, Nigeria

*[a]olalekan.olayemi@kwasu.edu.ng, [a]isiakamuhammed2015@gmail.com, [b]Khaled.alfarhany@qu.edu.iq, [c]mohammedff.hasan@qu.edu.iq, [d]muneer.ismael@uobasrah.edu.iq, [e]sunday.oyedepo@covenantuniversity.edu.ng

Keywords: Darcy number, Modified Rayleigh number, Natural convection, Porous medium.

Abstract. The natural convection around a heated trapezoidal block of different sizes positioned centrically in a larger trapezium has been investigated numerically. The annulus between the trapeziums is occupied by porous media. The sides of the inner trapezium are heated to a fixed temperature and the slanted walls of the outer trapezium are isolated thermally. In contrast, its upper and lower walls are heated uniformly. The pertinent dimensionless equations were solved with COMSOL Multiphysics 5.6. The parameters considered are modified Rayleigh number, Darcy number, and area ratio. The results of this study are shown as isothermal contours, stream functions, and average Nusselt number. The results show that increasing the modified Rayleigh number improves heat transfer; however, the response of the thermal profiles to area ratio increment depends on the range of Darcy number considered. This study finds application in ingot treatments and microchannel cooling, among others.

Introduction

The problem of convective heat transfer in a porous enclosure is a shining area of investigation in engineering due to its industrial significance. Embedded rods in a porous medium are of great interest in the heat treatment of ingots because their metallurgical properties and the time taken to produce them are widely affected by natural heat transfer. Thus, such a problem has received notable efforts of scientific research [1-5]. Fontana et al. [6] worked on the fluid flow powered by buoyancy forces in a trapezoidal enclosure with two baffles and noticed how the flow pattern is almost independent of inclination angle; however, an increase in inclination angle occasioned the enhancement of heat transfer. Hussein et al. [7] researched the density gradient induced flow in a triangular-roofed-rectangular cavity with insulated strips fitted in the center. It was noted that Rayleigh number impacts positively on heat transport enhancement. Abood [8] experimentally examined natural convective flow in a porous medium trapezoid. It was opined that increasing aspect ratio and modified Rayleigh number affected heat transfer coefficients positively. Buoyancy initiated flow in a trapezoidal enclosure whose vertical sides were under isothermal heating whereas the inclined walls were cooled was analyzed numerically by Al-Makhyoul [9]; they recognized that the average Nusselt number rises as the Rayleigh number is raised but decreases as baffle length and the number of baffles increase. Also, Olayemi et al. [10] also considered the influence of Rayleigh number in a buoyancy induced flow and their submission is in congruence with the view of [9]. Bejan [11] studied free convective flow in a porous vertical enclosure and opined that Rayleigh number dictated the accuracy of the Weber Method and that the heat transferred is enhanced by increasing Rayleigh number. Moukalled and Darwish [12] numerically analyzed convective fluid flow in a partitioned trapezoidal cavity. They discovered that the baffles reduced the rate of heat transfer, however, heat transfer increased with rising Prandtl number. Das et al. [13] numerically studied natural convection in non-square shapes; they showed that aspect ratio and baffles' presence along the walls of trapezoidal cavities investigated enhanced temperature and flow distributions.

Cheong et al. [14] considered the influence wall inclination has on buoyancy flow in a trapezoidal tilted-porous enclosure. Results from their investigation indicated that enclosure shape influenced heat transfer patterns. Hussein [15] investigated heat transfer solely occasioned by buoyancy force in a trapezoidal enclosure containing different fluids. They discovered that the method of transferring heat affects flow circulation; furthermore, the circulation strength increases as convection becomes more vigorous. Miroshnichenko et al. [16] numerically experimented on convective heat transfer in a vented nanofluid-equipped trapezoidal enclosure. They reported that raising nanoparticle size improves heat transfer rate while the higher the Hartmann number, the lower the transport of heat. Similarly, the observation made by Olayemi et al. [17] in their study of the impact of nanofluid volume fraction on heat transfer aligns with that of [16]. Free convection flow was experimented on by Ventakadri et al. [18] in an enclosed trapezoidal area with radiation effects. They concluded that improvement in the radiation parameter and the Rayleigh number improved heat transfer.

Ventakadri et al. [19] simulated free convection fluid flow in a left-wall heated trapezoidal cavity and had a cold top wall with other walls kept insulated. Their investigation showed that Rayleigh number increment resulted in heat transfer augmentation. Ghalambaz et al. [20] gave an account of the impact of viscous dissipation on free convection in a square enclosure with nanofluid. It was opined that the Nusselt number on the cold wall increased but decreased along the hot wall when there was a rise in viscous dissipation. Walker and Homsy [21] numerically studied density gradient propelled heat transport in a porous enclosure and reported that an increase in the Rayleigh number value at a given channel ratio caused a corresponding surge in heat transfer rate. Sheremet et al. [22] looked at simulating density gradient initiated flow in a porous trapezoidal enclosure which generated internal heat. The cavity walls were subjected to various thermal conditions. It was revealed that an increase in heat generation in the cavity resulted in an increase in thermal gradient at the cold wall but reduced the thermal gradient at the hot wall. In the same vein, Olayemi et al. [23] evaluated the impact of internal heat generation and absorption in an MHD flow in a square enclosure. Their submission corrobates the report of [21] on the significance of heat generation on the augmentation of heat transport.

Esfe et al.[24] numerical experiments on density variation initiated heat transport in a square enclosure containing nanofluid having variable temperature distributions on the left boundary. It was submitted that wave number and tem perature distribution increments on the left wall aided the improvement in the mean value of the entropy generated. An experimental analysis was carried out by Hossain et al. [25] on the convective flow of heat in a trapezoidal configuration containing an embedded triangular block; they demonstrated that heat transfer augmentation relies largely on the embedded uniformly heated triangular block. Gholizadeh and Nikbakhti [26] investigated natural convection heat transfer in a partially heated trapezoidal cavity. They discovered that the heat transfer augmentation rate depends on the positioning of the source of heat. Akter and Pervin [27] analyzed convective heat flow in a trapezoid housing a centrally placed rectangular block. They upheld that the rate at which heat is augmented depends on Rayleigh and Hartmann numbers, and fluid type.

Baytas and Pop [28]considered a tilted porous trapezoidal configuration with a free convective flow mechanism. Their reports evidenced that Rayleigh number increment enhances the convective flow regime. Beckermann et al. [29] numerically evaluated buoyancy flow in a vertical porous medium. They showed that an inverse relationship exists between the heat transferred and Darcy number. Radhi [30] examined convection heat flow numerically in a trapezoidal porous enclosure containing a centrally placed square. They submitted that the wall conditions determine the flow and heat distribution pattern. In addition, the flow intensity is enhanced by improving Rayleigh number. Lam et al. [31]employed numerical and experimental methods to investigate natural convective fluid flow in a tilted trapezoid. The submission made was that inclination angle increment resulted in a decrease in the average Nusselt number. Saha [32] studied a differentially heated tilted porous trapezoid immersed in a porous medium. They concluded that the enclosure aspect ratio increase led to an enlargement of the thermally stratified region.

Sivasankara et al. [33] numerically analyzed heat transfer in a tilted porous triangular enclosure due to buoyancy force. In their investigation, the cavity walls were subjected to linear and sinusoidal thermal boundary conditions. They observed that the sinusoidal thermal boundary condition resulted in more heat transfer augmentation than the linear wall condition. Olayemi et al. [34] also considered heat transfer in a sinusoidally heated square enclosure where it was affirmed that the mid-plane velocity was highest at 40% of the enclosure height. Basak et al. [35] simulated density gradient supported flow in a tilted porous trapezoidal enclosure; it was reported that the highest heat transfer enhancement happened at a zero-degree inclination angle. Basak et al. [36] numerically studied the impacts of uniform and uneven heating at the base of a porous trapezoid. They discovered that uniform heating provided a better heat transfer rate occasioned by the low gradient in temperature. Adibi et al. [37] compared the heat transfer abilities of air and lubricating oil in a porous cavity numerically. It was confirmed that the generated flow when air was used as the working fluid is stronger than oil.

Hossain and Wilson [38] analyzed heat transport by convection in a rectangular porous non-isothermal enclosure. It was revealed that porosity increase resulted in decreased fluid flow at the dominant vortex region which led to a cut-down in the rate at which heat was augmented along the boundaries of the enclosure. Sompong and Witayangkurn [39] investigated free convection in a trapezoid having a wave-like top surface; they submitted that Rayleigh and Darcy numbers affect flow intensity and temperature distribution. While studying convective fluid flow in a tilted trapezoid having a porous medium with both heated and cold side walls, Varol et al. [40] figured out that in contrast with the sidewall inclination angle, the trapezoid inclination angle enabled improved heat transport augmentation. Varol [41]worked on the numerical examination of natural convection, which took place inside a partitioned saturated porous trapezoidal cavity. The walls were conditioned to different thermal boundaries; they reasoned that at both low Rayleigh number and thermal conductivity ratio, the heat was transferred mainly by conduction, increasing the partition thickness scales down the strength of heat transfer. Alsabery et al. [42] numerically experimented on convective flow in a nanofluid porous trapezoid; it was reported that nanoparticle addition resulted in a buoyancy increase. Alomari et al. [43] considered the effects of MHD natural convection on a trapezoidal cavity filled with hybrid nanofluid. Their results showed that the Nusselt number increases with the Rayleigh number and the volume fraction while it decreases with the Hartmann number.

Based on the thorough literature search conducted, few studies on natural convective heat transmission in a trapezium filled with porous media have been conducted. Furthermore, no previous work had been reported on the numerical analysis of natural convection in a concentric trapezoidal enclosure filled with porous media. As a result, the current study aims to fill in these knowledge gaps. This work has various practical applications viz heat treatment of ingots, nuclear reactor technology, space, and cabinet heating. Finally, in the academia, experimenalists in related areas would find information contained in this study very handy.

Methodology

Physical Model Description

Fig. 1 presents a two-dimensional physical model and the coordinate system utilized in the current study. The model is made up of a small solid trapezium placed centrally in a large trapezium with an area ratio $AR = \frac{A_i}{A_o}$; where A_i is the area of the inner trapezium and A_o is the area of the outer trapezium. The annular space created by virtue of the presence of the inner trapezium is filled with a porous medium. The end effect in the z-direction is presumed to be inconsequential; therefore, the fluid flow and thermal profiles are 2-dimensional. Additionally, the flow in the enclosure is presumed to be laminar and agrees with the Darcy-Brinkman model. The boundaries of the inner trapezium are fixed at a temperature of T_h, the slanted walls of the outer trapezium are taken to be adiabatic while its upper and lower horizontal walls are maintained at fixed temperatures of $T_c + (T_h - T_c)\sin(\pi x/L)$ and $T_h + (T_h - T_c)\sin(\pi x/L)$ respectively. Except for density which follows the Boussinesq approximation, the fluid properties are presumed as constant; and fluids in contact with stationary boundaries are assumed to have zero velocity.

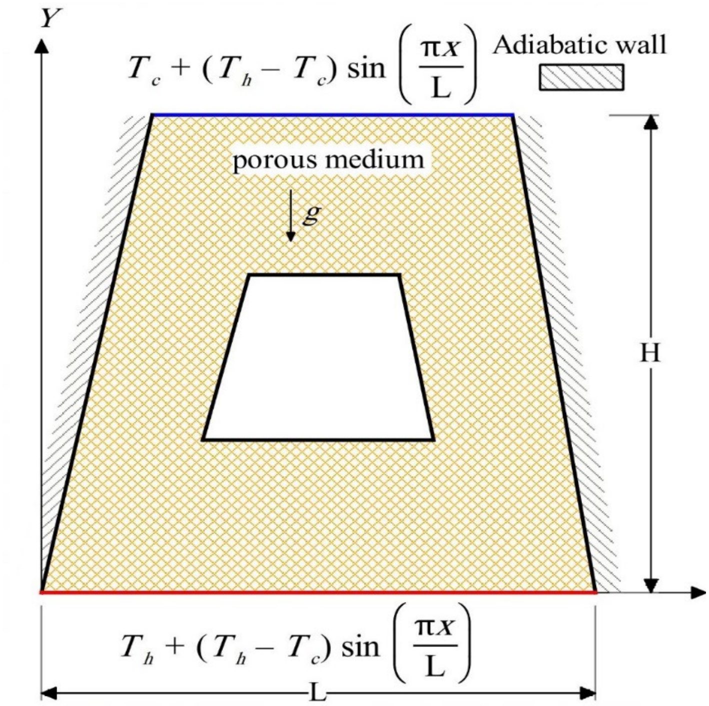

Figure 1: Physical Model.

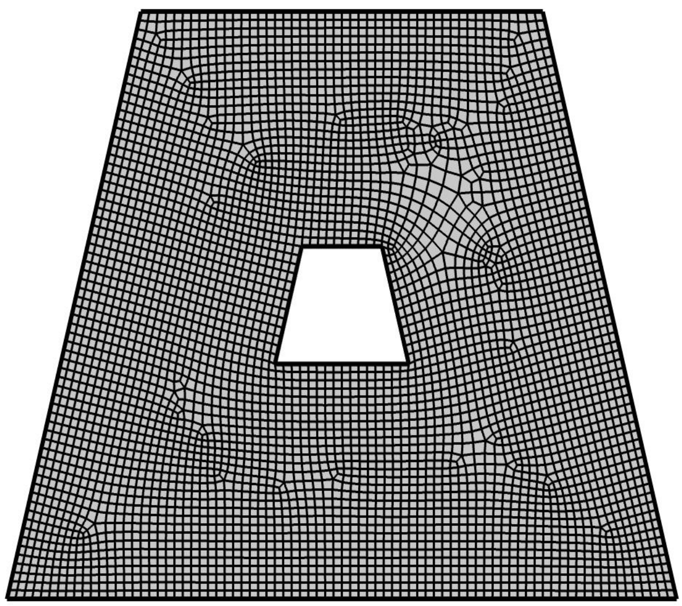

Figure 2: Mesh Distribution.

Governing equations

The dimensional equations that are relevant to the current problem are as defined by Kumar [44]:
Continuity:

$$\frac{\partial u}{\partial x}+\frac{\partial v}{\partial y}=0 \tag{1}$$

Momentum transport equations:
x -direction:

$$\rho\left(u\frac{\partial u}{\partial x}+v\frac{\partial u}{\partial y}\right)=-\frac{\partial p}{\partial x}+\mu\left[\frac{\partial^2 u}{\partial x^2}+\frac{\partial^2 u}{\partial y^2}\right]-\frac{\mu u}{K}-\frac{C_f\rho u^2}{\sqrt{K}} \tag{2}$$

y −direction:

$$\rho\left(u\frac{\partial v}{\partial x}+v\frac{\partial v}{\partial y}\right)=-\frac{\partial p}{\partial y}+\mu\left[\frac{\partial^2 v}{\partial x^2}+\frac{\partial^2 v}{\partial y^2}\right]-\frac{\mu v}{K}-\frac{C_f\rho v^2}{\sqrt{K}}+\rho g\beta(T_h-T_c) \tag{3}$$

Energy transport equation:

$$u\frac{\partial T}{\partial x}+v\frac{\partial T}{\partial y}=\alpha\left(\frac{\partial^2 T}{\partial x^2}+\frac{\partial^2 T}{\partial y^2}\right) \tag{4}$$

The non-dimensional equations that are relevant to the current problem are as defined by Kumar [44]:
Continuity:

$$\frac{\partial U}{\partial X}+\frac{\partial V}{\partial Y}=0 \tag{5}$$

Momentum transport equations:

X-direction:

$$U\frac{\partial U}{\partial X}+V\frac{\partial U}{\partial Y}=-\frac{\partial P}{\partial X}+Pr\left[\frac{\partial^2 U}{\partial X^2}+\frac{\partial^2 U}{\partial Y^2}\right]-\frac{PrU}{Da}-\frac{U^2C_f}{\sqrt{Da}} \tag{6}$$

Y-direction:

$$U\frac{\partial V}{\partial X}+V\frac{\partial V}{\partial Y}=-\frac{\partial P}{\partial Y}+Pr\left[\frac{\partial^2 V}{\partial X^2}+\frac{\partial^2 V}{\partial Y^2}\right]-\frac{PrV}{Da}-\frac{V^2C_f}{\sqrt{Da}}+\frac{Ra_mPr\varphi}{Da} \tag{7}$$

Energy transport equation:

$$U\frac{\partial \varphi}{\partial X}+V\frac{\partial \varphi}{\partial Y}=\frac{\partial^2 \varphi}{\partial X^2}+\frac{\partial^2 \varphi}{\partial Y^2} \tag{8}$$

Transformation parameters

$$X=\frac{x}{L},Y=\frac{y}{L},AR=\frac{A_i}{A_o},U=\frac{uL}{\alpha},V=\frac{vL}{\alpha},\varphi=\frac{T-T_c}{T_h-T_c},P=\frac{pL^2}{\rho\alpha^2},Pr=\frac{\upsilon}{\alpha} \tag{9}$$

$$Da=\frac{K}{L^2},\qquad Ra_m=\frac{\rho g\beta(T_h-T_c)KL}{\mu\alpha} \tag{10}$$

Solution Technique

The present study was implemented with COMSOL 5.6 software. The Heat transfer and fluid flow environment were used to simulate the model adopted for the study. The first step in the simulation involved selecting the model wizard and model dimension to be investigated. The physics governing the model under investigation (heat transfer in fluid and laminar flow) was then established. The required parameters for the study were inputted into the parameters' settings window under the global definitions node. The geometry used in the investigation was produced by selecting a polygon under the geometry node, and then the coordinates of the geometry were inputted. After that, the Boolean operation was used to subtract the inner trapezium from the outer trapezium to produce the annulus where fluid flow took place. Under the laminar flow-node, the fluid properties were inputted; the initial conditions, wall conditions, and the appropriate expressions for the volume force were all specified. Furthermore, the fluid properties and the wall thermal boundary conditions were specified under the heat transfer in the fluids node. The mesh was produced using the free quadrilateral mesh option. Under the study 1 node, the parametric sweep was added, this was used to conduct a parametric study of salient parameters like AR, Ra_m and Da . Interpolation function $(P_1 + P_1)$ was used to approximate the meshed-domain whereas the linear finite element method was used to discretize the temperature field . In order to take care of the convective term in the momentum equations, the mesh employed for the simulation was finely resolved. Artificial diffusion term was used to resolve local instabilities. while the segregated parametric solver was employed for the heat transfer and fluid flow variables. Biconjugate gradient stabilized iterative method solver was employed for the heat transfer and fluid flow modules of the commercial software used, Selimefendigil et al. [45].

In the present investigation, grids of different sizes were used for the geometry considered to observe their implications on the results of the average Nusselt number of the heated lower solid boundaries of the outer trapezium. Based on the results of the numerical experiments conducted as shown in Table 1, the grid size of 100×100 was chosen since the error is closest to the least error but with less computer run time than that of the 120 × 120 grid size shown in Fig. 2.

Table 1: Grid sensitivity test of the mean Nusselt number ($\overline{Nu}$) on the lower outer horizontal wall of the heated trapezium for $Ra_m = 10^3$, $AR = \frac{1}{3}$, $Da = 10^{-5}$, and $C_f = 1$.

Mesh Dimension	$\overline{Nu}$	% error
30 by 30	4.7821	----
50 by 50	4.9348	3.19
70 by 70	5.0487	2.31
90 by 90	5.1344	1.70
100 by100	5.1741	0.77
120 by120	5.2102	0.70

Evaluation of Nusselt number

The heat transport along the heated wall can be calculated by assessing the Nusselt number along the wall. According to Radhi [30] and Adegun et al. [46] and Olayemi et al. (47), the equations for the evaluation of the local and average Nusselt numbers can respectively be cast as:

$$Nu_L = -k\frac{\partial \varphi}{\partial n} \tag{10}$$

$$\overline{Nu} = \frac{1}{S}\int_0^S Nu_L \, dS \tag{11}$$

Stream function

The motion of the fluid is reckoned with the aid of stream function (Ψ), which is calculated from streamline contours that represent the flow fields within the cavity and is formed by making use of the components of velocities U and V as follows: [48-51]

$$U = \frac{\partial \Psi}{\partial Y}, \qquad V = -\frac{\partial \Psi}{\partial X} \tag{12}$$

The formulation of the stream function equation is therefore given as:

$$\frac{\partial^2\Psi}{\partial X^2}+\frac{\partial^2\Psi}{\partial Y^2}=\frac{\partial U}{\partial Y}-\frac{\partial V}{\partial X} \tag{13}$$

According to stream function definitions, anticlockwise circulation has a positive value, whereas clockwise circulation has a negative value.

Validation of Results

To validate the COMSOL Multiphysics 5.6 code employed in the current analysis, the average Nusselt numbers along the heated horizontal wall of a porous square enclosure obtained in the present study are compared in Table 2 and Table 3 with those of previous studies, and the comparisons agree quite well.

Table 2: Comparison of the current results with Ghasemi et al.[52] at the free magnetic field (Ha = 0).

Ghasemi et al. [52]			Present	
Φ	$\lvert\Psi\rvert_{max}$	Nu_{avg}	$\lvert\Psi\rvert_{max}$	Nu_{avg}
0	11.053	4.738	11.087	4.7489
0.02	11.313	4.820	11.352	4.8323
0.04	11.561	4.896	11.604	4.9105
0.06	11.801	4.968	11.846	4.9836

Table 3: Comparison of the values of the average Nusselt number along the heated wall of a porous square enclosure in the current study with those of previous studies [21, 53, 54]when $Pr = 0.71$ and Da=10^{-5}.

Ra_m	Walker and Homsy [21]	Moya et al. [53]	Malomar et al. [54]	Present Study
10	-	1.065	1.078	1.076
100	3.100	2.800	3.120	3.029
1000	12.960	-	15.600	12.536

Results and Discussion

This section presents the results of the effects of modified Rayleigh number $(10 \le Ra_m \le 1000)$, area ratio of the concentric trapezium $\left(\frac{1}{5} \le AR \le \frac{1}{3}\right)$ and Darcy number $(10^{-5} \le Da \le 10^{-2})$ on heat transfer and fluid flow dynamics inside the domain probed.

Figs. 3-5 show the implications of modified Rayleigh number (Ra_m) and Darcy number (Da) for area ratio (*AR)* values of $\frac{1}{5}$, $\frac{1}{4}$, and $\frac{1}{3}$ respectively. For all the modified Rayleigh and Darcy numbers considered, there are six cells distributed around the annulus of the concentric trapezoid, with the sizes of the cells ranging from small to big from top to bottom. The fluid flow is symmetric about the vertical axis of the center of the enclosure. Each of the adjacent cells rotates in an alternative direction, which can be explained by the following. Firstly, it should be noted that the coldest situations in the domain are the upper corners, while the hottest situation is the mid-span of the lower wall of the cavity. Based on these situations, the rising fluid from the lower wall will be resisted by the inner trapezium while there are free paths to the fluid rising from both edges of the lower wall. This condition results in a clockwise cell at the lower-left corner and an anticlockwise cell at the lower right corner. Moreover, close to the upper wall, the fluid pursues the colder regions, i.e., the upper corners; thus, the cells rotate similarly to the lowest cells. Hence, the identical rotation of the upper and lower cells on either side of the inner trapezium will guide the fluid between these two cells to rotate in an alternative manner. Due to the available space, the lower cells are stronger than the upper cells. The plots in Fig. 3 show that when Da=10^{-5}, the maximum stream function (Ψ) increases from 0.05 at Ra_m=10 to 2.6 when Ra_m=1000; this occurrence is occasioned by buoyancy force increase due to the rise in natural convective forces at constant values of other parameters; which is highest at the extreme importance of Ra_m. On the other hand, the figure shows that the maximum stream function reduces with increasing Da at a constant Rayleigh number. For instance, at Ra_m of 1000, Ψ_{max} reduces from 2.6 to 0.61 at Da = 10^{-5} and 10^{-2} respectively. As expected, the same trend was observed for different AR values, as displayed in Fig. 4. The highest value of the stream function was realized at the peak value of Ra_m of 1000 and at the least value of Da of 10^{-5} and it is equal to 2.2.

From Figs. 3 and 4, for fixed values of Ra_m and Da, it was noticed that stream function values reduce as AR increases in value due to the obstacle size increment, which restricts the circulation of the vortices. This difference between values of stream functions increases with the increase in the values of both Ra_m and Da and attains a maximum value at $Ra_m$of 1000 and Da of 10^{-2}, where Ψ_{max} is 0.61 and 0.55 respectively for Fig. 3 and Fig. 4. This difference is further increased with an increase in *AR,* as seen in Fig. 5.

Fig.6 shows the impact of Ra_m and Da on isotherms at a fixed value of AR of 1/5. The results show that the isotherms are not sensitive to Da changes while they slightly squeeze and become denser close to the lower wall with the increase in the value of Ra_m. This behaviour is due to the intensification of natural convection. The contours of the isotherms become less dense as the size of the trapezoidal obstacle increases, as seen in Figs. 7 and 8. The physical explanation for the observed trend is that an increase in area ratio (AR) of the geometry brought about a drop in the strength of the circulation, and hence the convective strength is also decreased. The plots in Figs. 9 and 10 summarize the impacts of AR and Ra_m at fixed Darcy number (Da = 10^{-5}) on the flow and heat profiles, and it affirms the previous trend of the effects of area ratio (*AR)* and Ra_m on flow strength and heat transfer profile within the annulus.

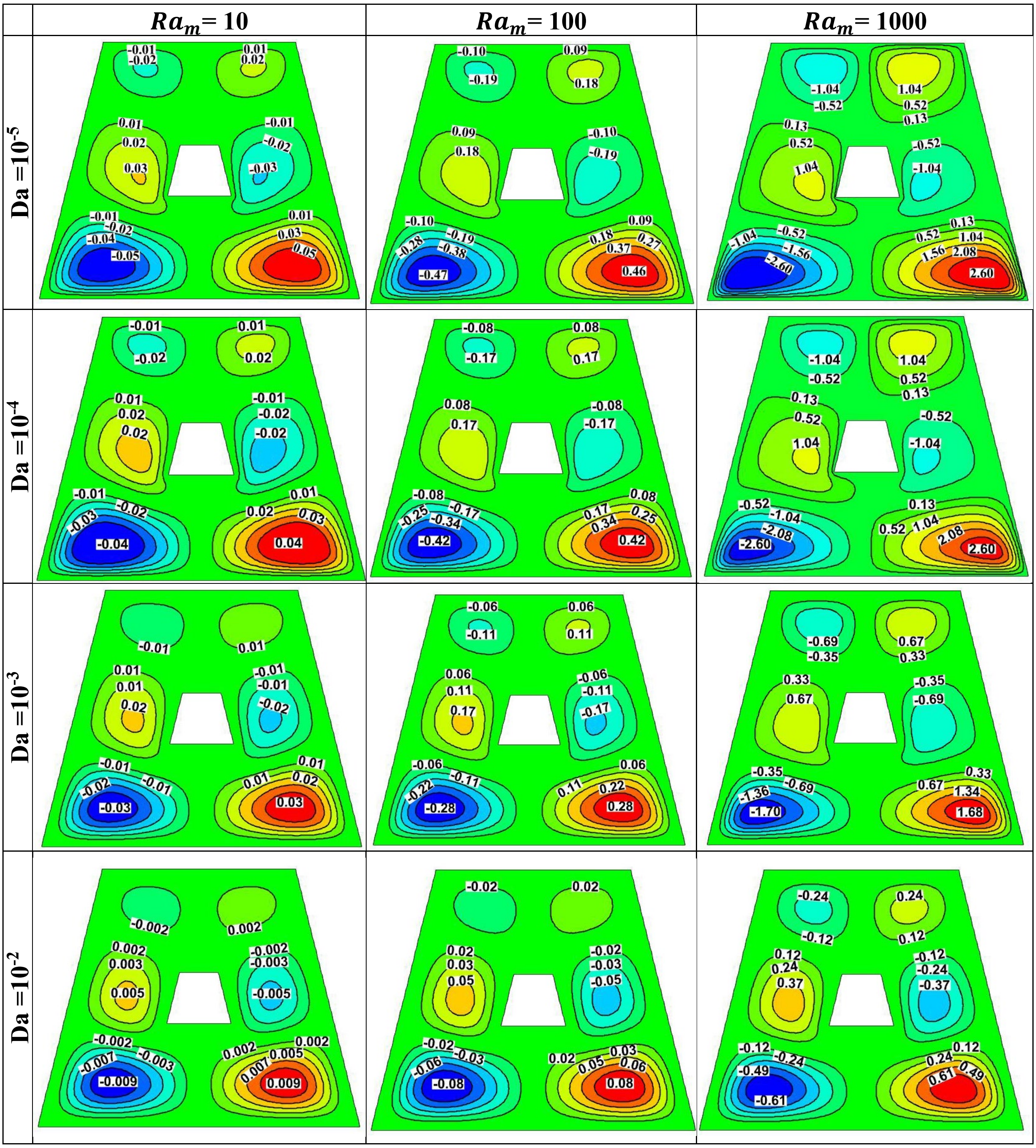

Figure 3: The effects of Ra_m and Da on stream function at AR =1/5.

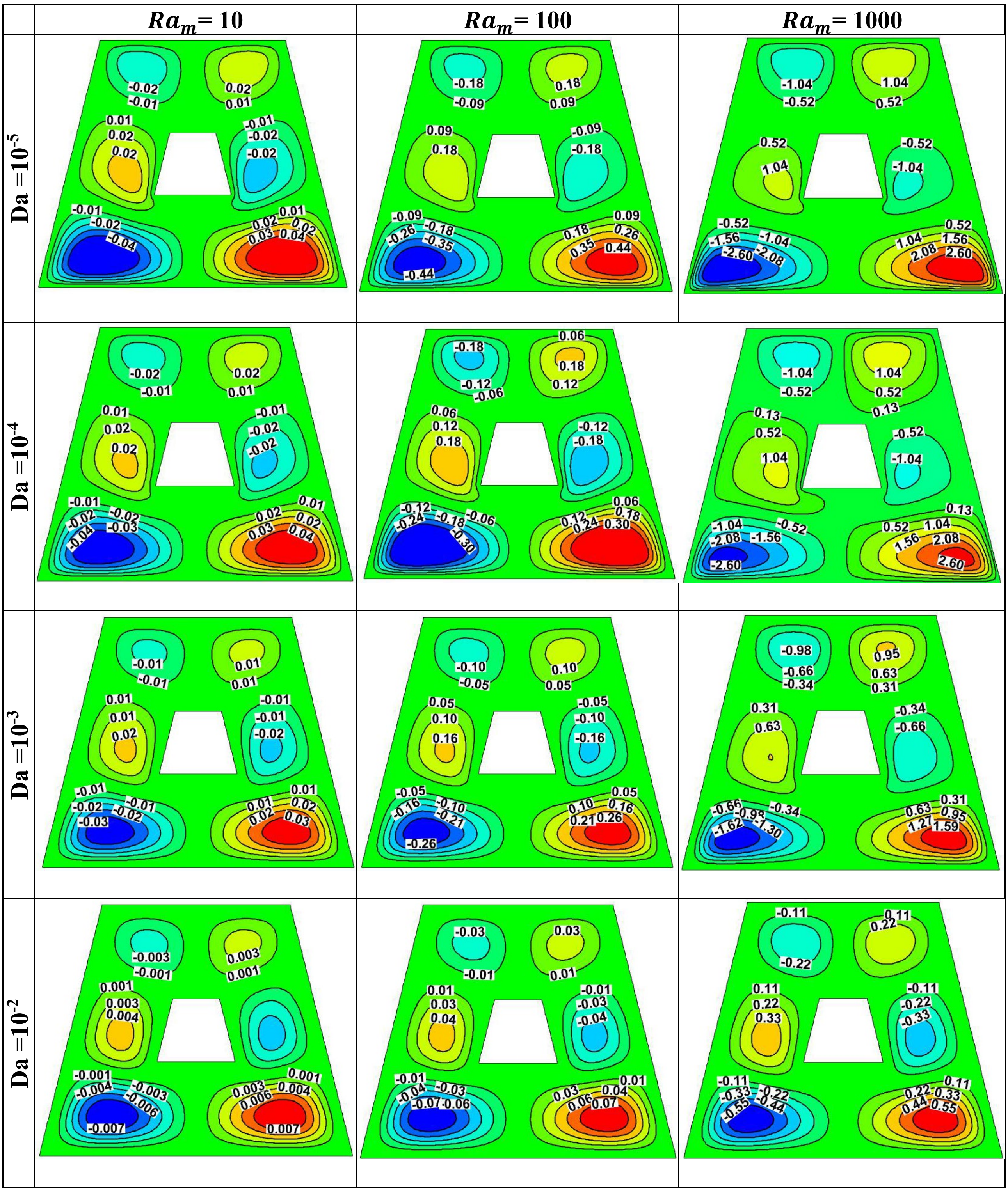

Figure 4: The effects of Ra_m and Da on stream function at AR =1/4.

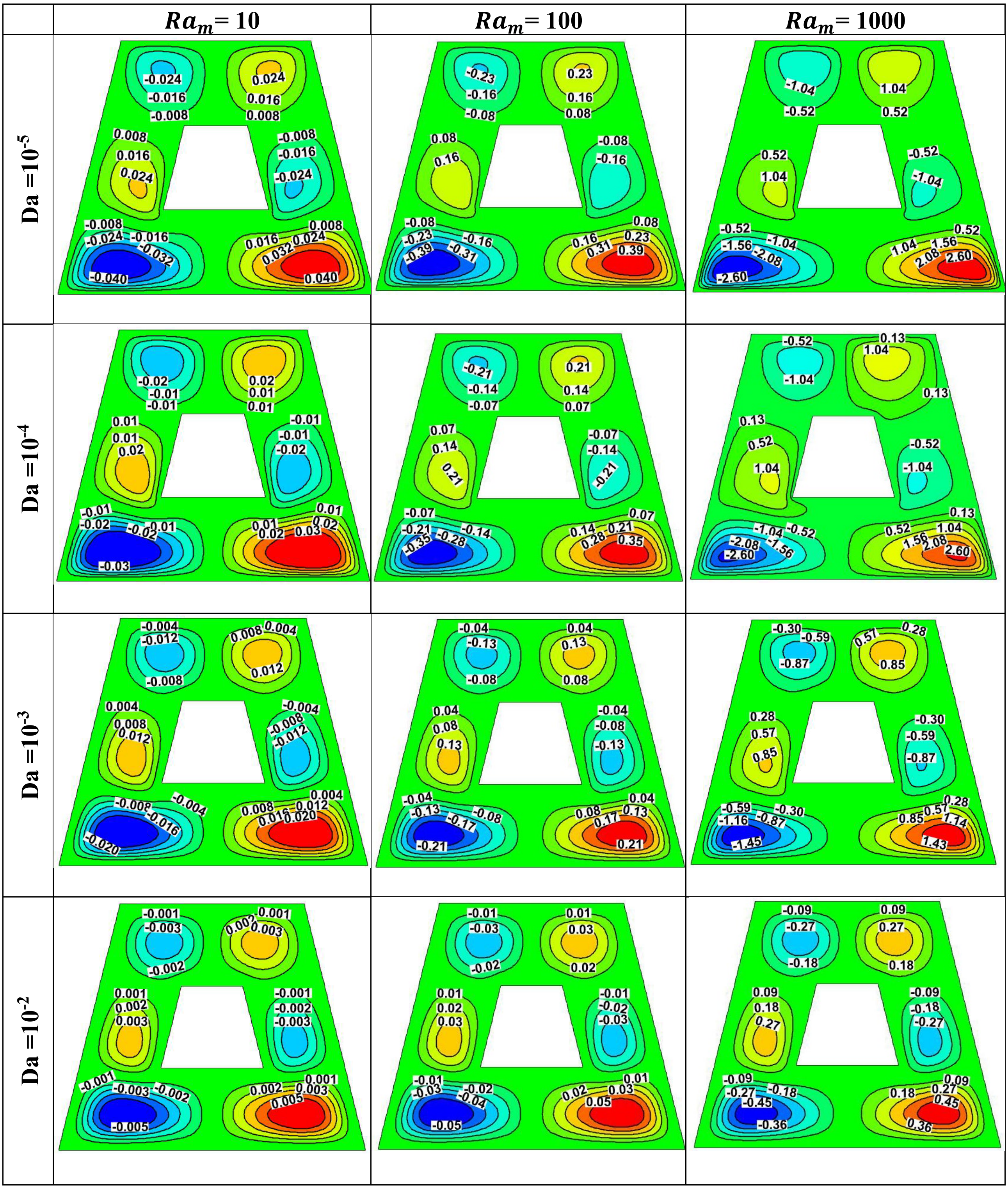

Figure 5: The effects of Ra_m and Da on stream function at AR =1/3.

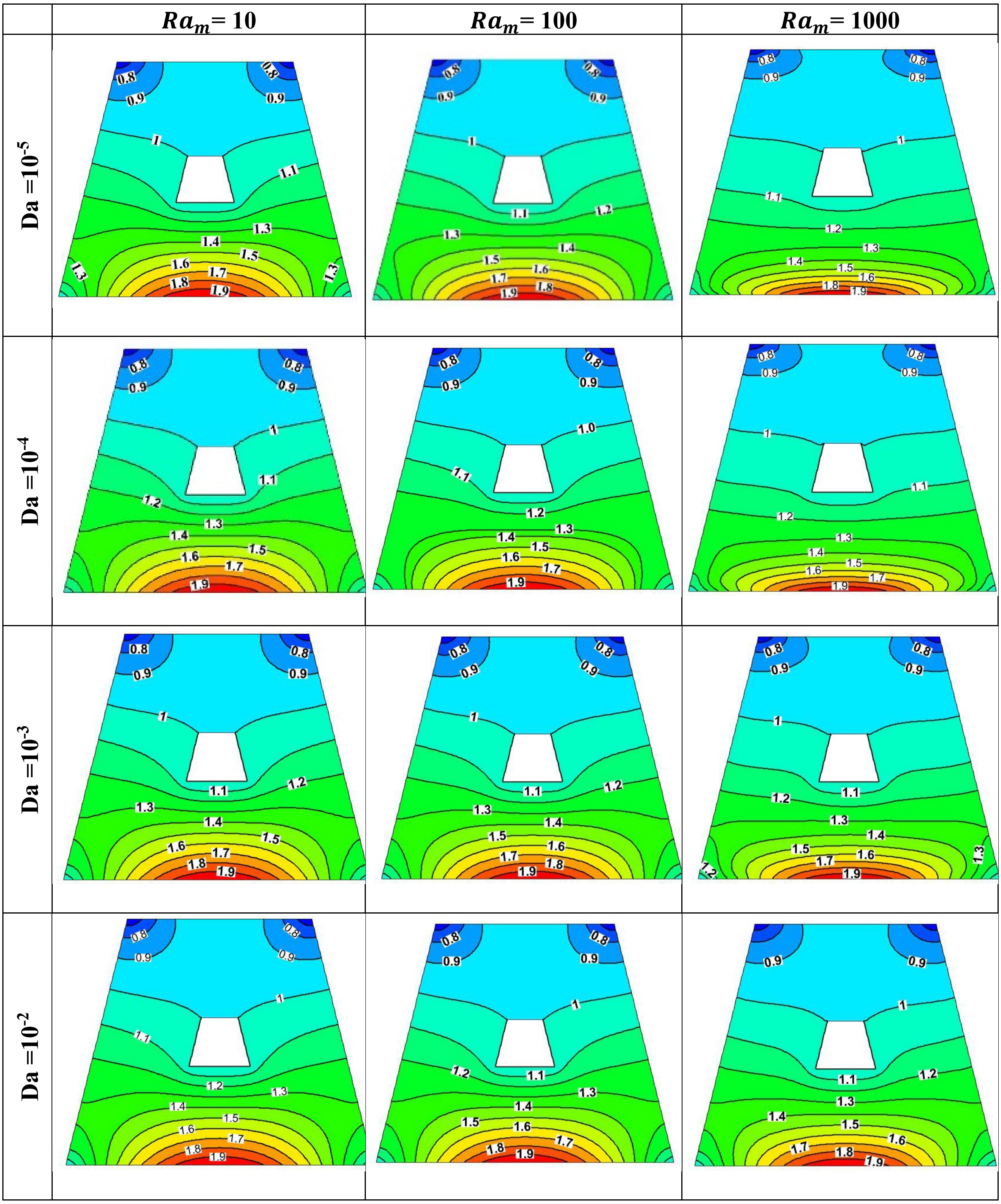

Figure 6: The effects of Ra_m and Da on isotherms at AR =1/5.

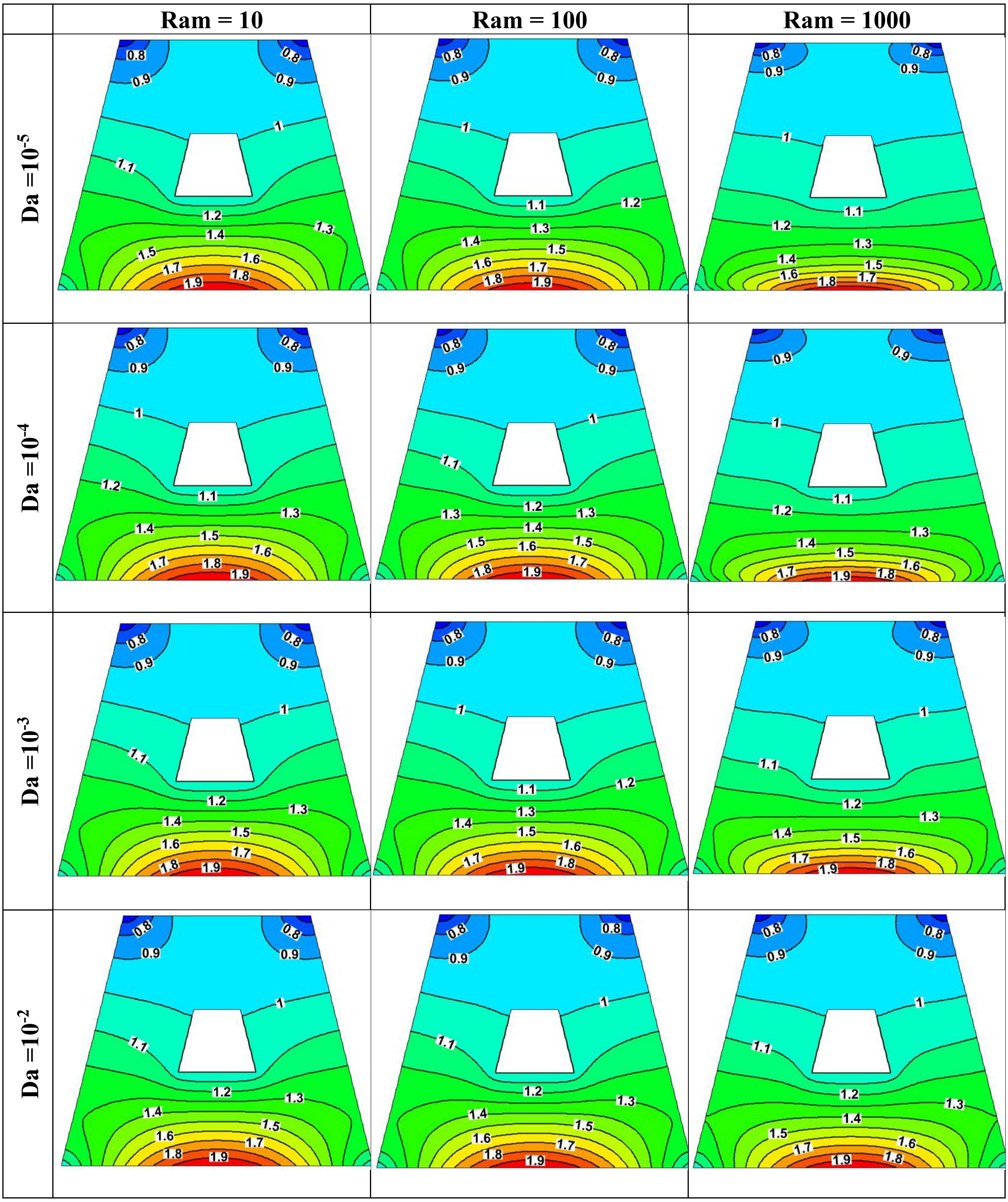

Figure 7: The effects of Ra_m and Da on isotherms at AR =1/4.

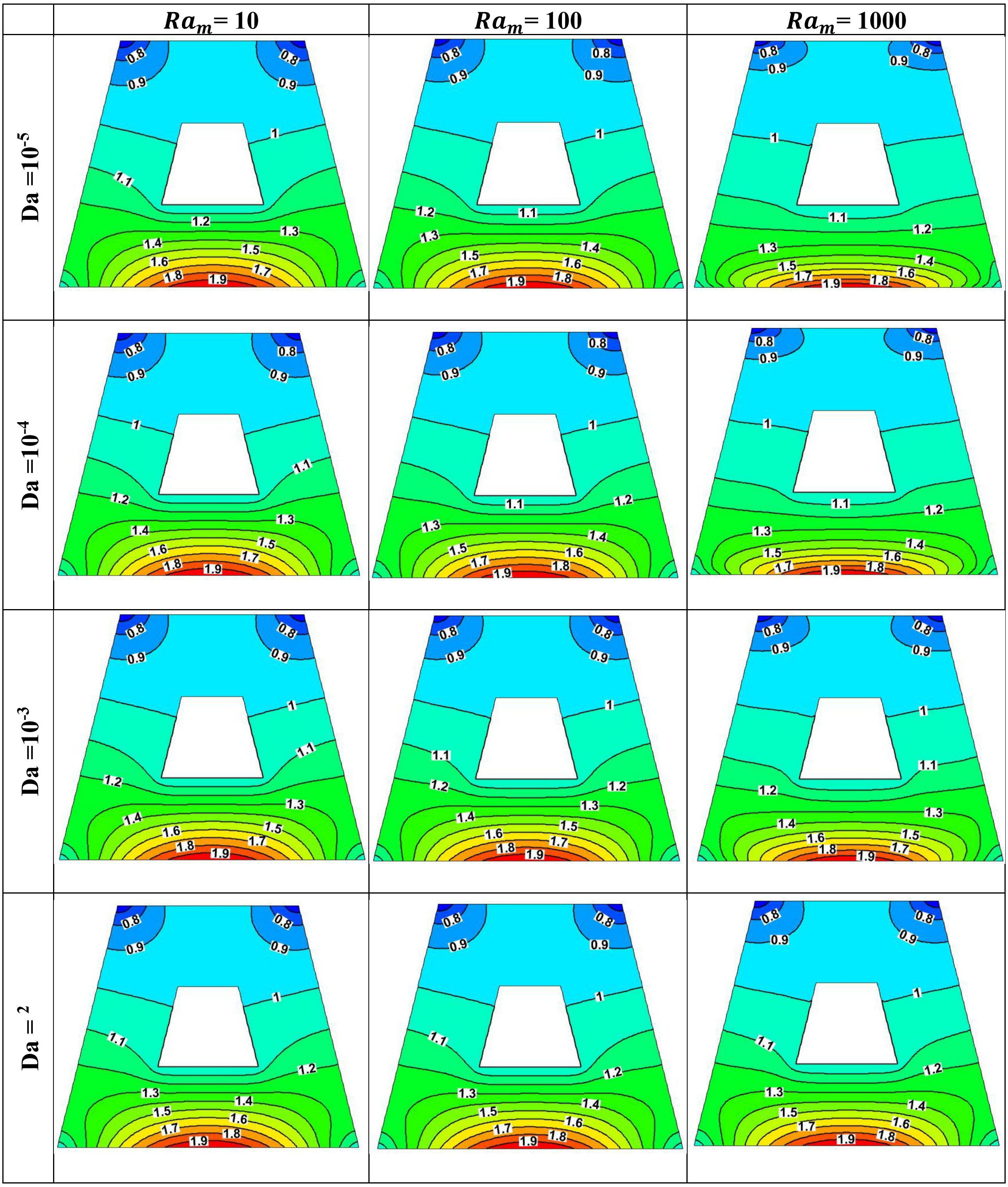

Figure 8: The effects of Ra_m and Da) on isotherms at AR =1/3.

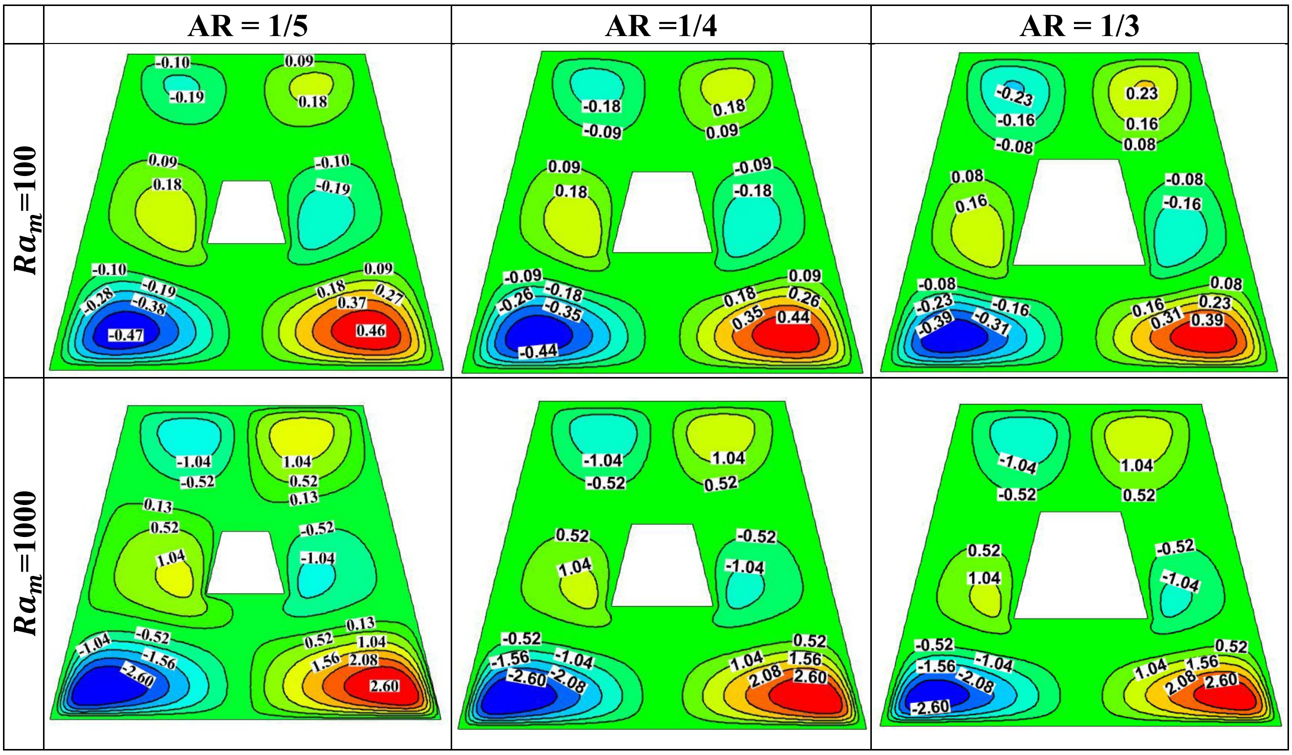

Figure 9: Stream function for varying AR at *Da=10*$^{-5}$, for Ra_m=100, and Ra_m=1000, respectively.

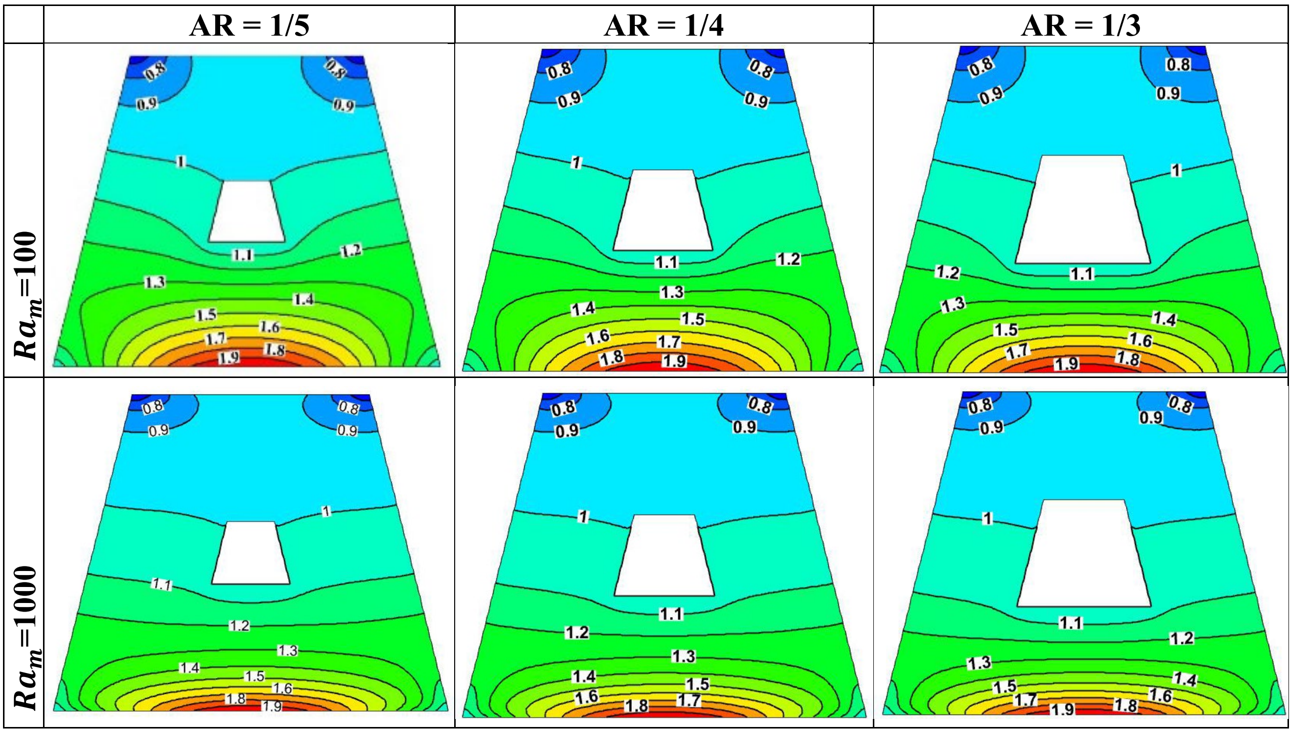

Figure 10: Isotherm for varying AR at fixed value of *Da*=10^{-5} at Ra_m=100, and Ra_m=1000.

Fig.11 depicts the plots of the average Nusselt number ($\overline{Nu}$) at the bottom wall of the outer trapezium against modified Rayleigh (Ra_m) for various area ratios at $Da = 10^{-5}$. The plots reveal that the average Nusselt number picks up as the modified Rayleigh number increases due to an increase in the buoyancy effect. Furthermore, Fig. 11 shows that as the size of the inner trapezium increases, the rate of heat transfer augmentation increases due to increased heating arising from the contribution of the warm walls of the inner trapezium. In addition, beyond Ra_m of 850 and AR of $\frac{1}{5}$, the heat transfer enhancement is almost insensitive to the size of the inner trapezium.

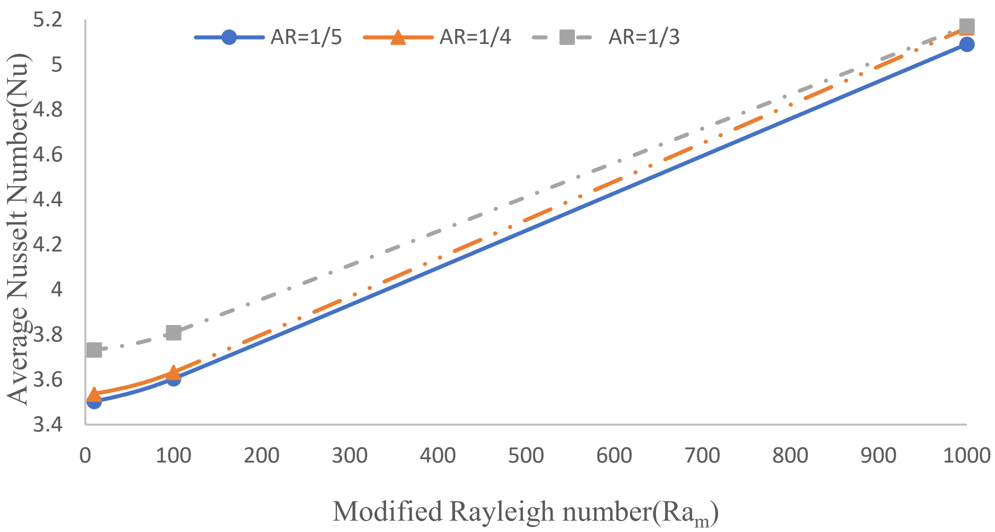

Figure 11: Average Nusselt number ($\overline{Nu}$) versus modified Rayleigh number (Ra_m) on the bottom wall of the outer trapezium for various Area ratios (AR) at $Da = 10^{-5}$, $C_f = 1$.

Fig. 12 presents the plot of the average Nusselt number along the lower wall of the outer trapezium against the modified Rayleigh number (Ra_m) for varied sizes of the inner trapezium at $Da = 10^{-4}$. The plots in Fig. 12 show that the average Nusselt number improves as the modified Rayleigh number increases. Also, for modified Rayleigh number in the interval of $10 \leq Ra_m \leq 850$, the average Nusselt number increases with an increase in the size of the inner trapezium. For $850 \leq Ra_m \leq 1000$, the rate of increase in heat transfer for area ratio in the interval of $\frac{1}{5} \leq AR \leq \frac{1}{4}$ is almost insignificant but becomes noticeable for $AR > \frac{1}{4}$. Furthermore, as Darcy number value increases from 10^{-5} to 10^{-4}, average Nusselt number decreases.

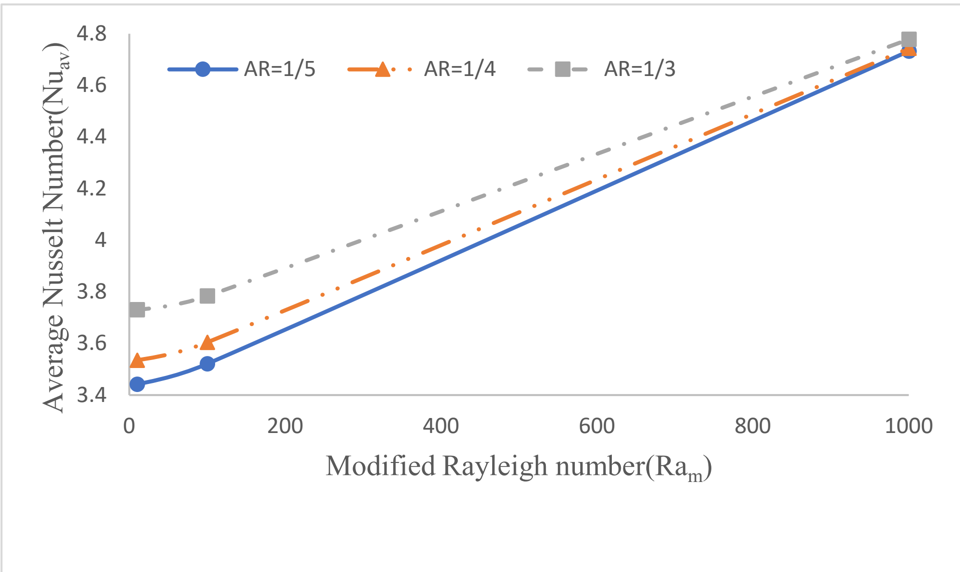

Figure 12: Average Nusselt number ($\overline{Nu}$) versus modified Rayleigh number (Ra_m) on the bottom wall of the outer trapezium for various Area ratios (AR) at $Da = 10^{-4}$, $C_f = 1$.

Fig. 13 presents the relationship between the rate of heat transfer and modified Rayleigh number for various values of AR at $Da = 10^{-3}$. The average Nusselt number increases with increasing Rayleigh number for all the sizes of the inner trapezium considered. The graphs also show that the average Nusselt number increases with an increase in the area ratio of the geometry. The plots also reveal a further reduction in the rate of heat transfer when Darcy number is increased from $Da = 10^{-5}$ to $Da = 10^{-3}$.

For Da of 10^{-2}, the plots of average Nusselt number versus modified Rayleigh number for area ratios of $\frac{1}{5} \leq AR \leq \frac{1}{3}$ are presented in Fig.14. The rate of heat transferred when $AR = \frac{1}{3}$ is significantly higher than the heat transfer rate when $AR = \frac{1}{4}$ for the range of the modified Rayleigh numbers considered. It is clear from the plots that the least heat transport enhancement happened at the peak value of the Da considered. However, Figs. 11 – 14 ascertain the reduction of the average Nusselt number with Da improvement, this can be explained by the fact that increasing Darcy number means scaling up the permeability value of the porous medium, which in turn enables stronger cells. Since the cells rotate in opposite fashions, then this imparts an adverse action on the convective flow in the annulus of the investigated model. This result is clearly illustrated in Fig. 15, where for the highest modified Rayleigh number considered, the average Nusselt number against Da plots for different sizes of the inner trapezium are depicted.

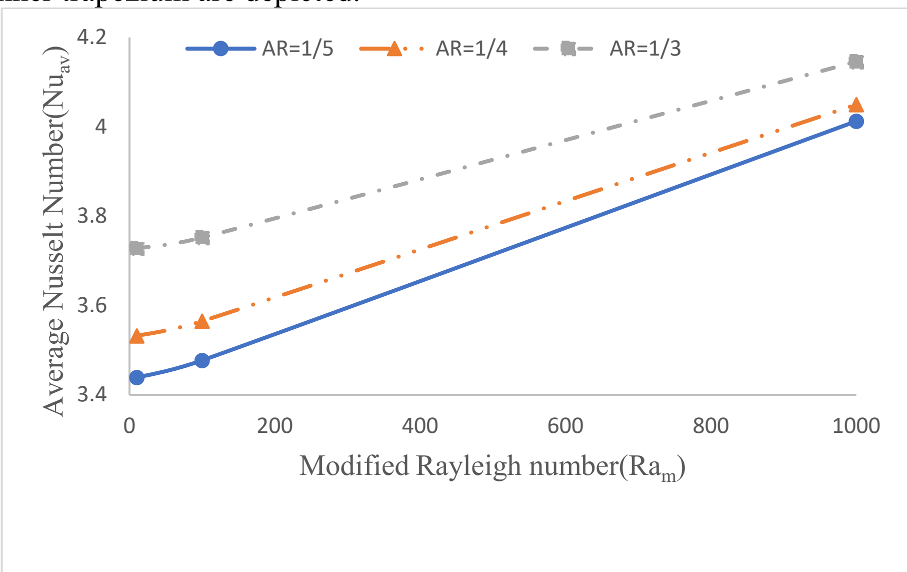

Figure 13: Average Nusselt number ($\overline{Nu}$) versus modified Rayleigh number (Ra_m) on the bottom wall of the outer trapezium for various Area ratios (AR) at $Da = 10^{-3}$, $C_f = 1$.

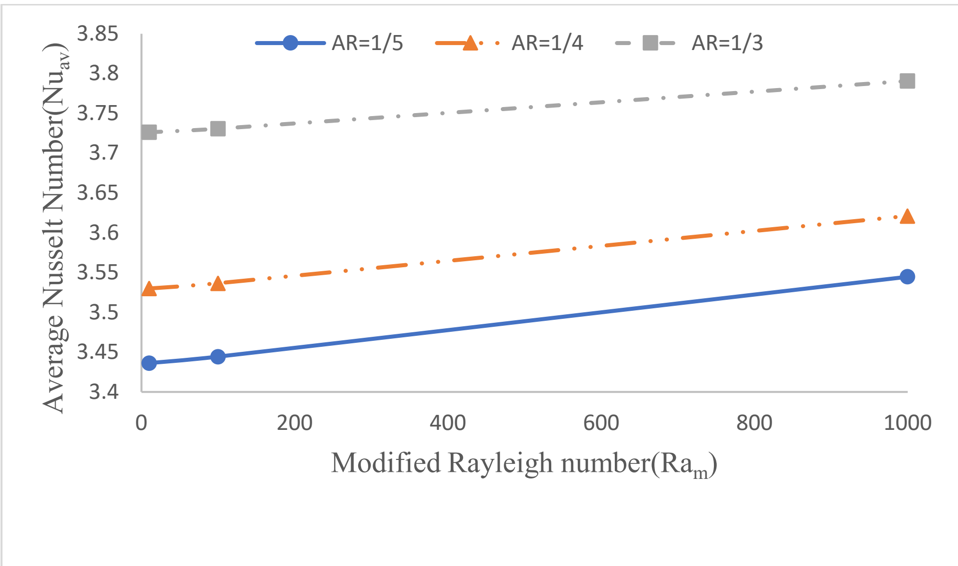

Figure 14: Average Nusselt number ($\overline{Nu}$) versus modified Rayleigh number (Ra_m) on the bottom wall of the outer trapezium for various Area ratios (AR) at $Da = 10^{-2}$, $C_f = 1$.

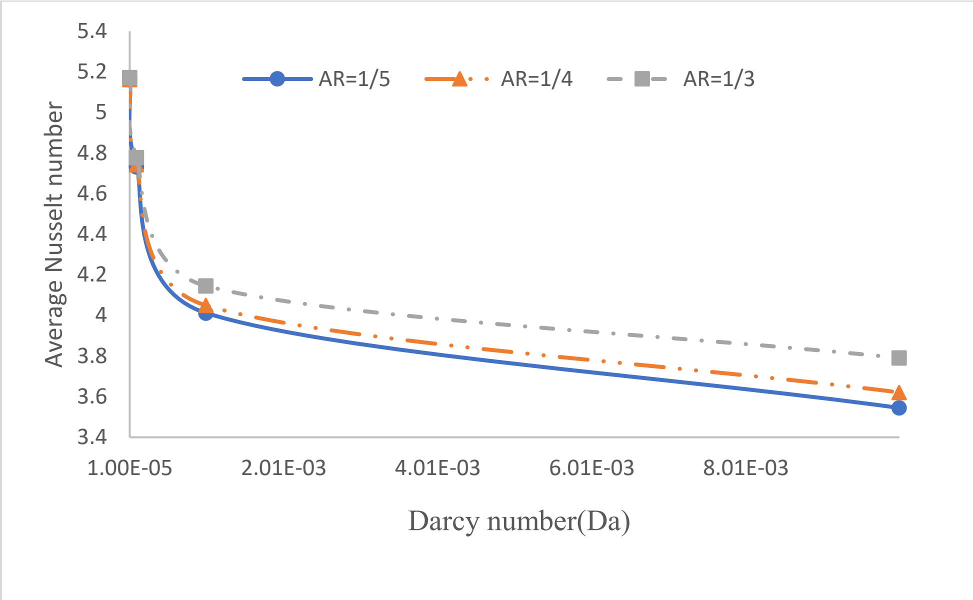

Figure 15: Average Nusselt number ($\overline{Nu}$) on the lower wall of the outer trapezium against Darcy number (Da) for different area ratios at Ra_m=1000, $C_f = 1$.

Comparison of the Streamfunction and Isotherms from the Current Investigation with those of Basak et al. [54]

Fig. 16 presents the comparison between the stream function and isothermal contour plots from the present investigation in the absence of the inner trapezium with those reported by Basak et al. [55]. The stream function and isotherms which are located on the top and bottom left in Fig. 16 are those from the current study while those located on the top and bottom right are respectively from the report of Basak et al. [55]. The slanted walls of each of the trapaziums in Fig.16 are kept at a cold temperature (T_c) and bottom horizontal wall is maintained at a constant hot temperutaure (T_h) while the top horizontal wall is isulated thermally. The porosity (Da) of the working fluid ($Pr = 0.71$) is 10^{-3}. The stream function and isothermal plots from the current investigation align with those reported by [55]. This comparison confirms the accuracy of the present code and therefore underscores its abillity to accurately predict flows in a porous concentric trapezoidal enclosures.

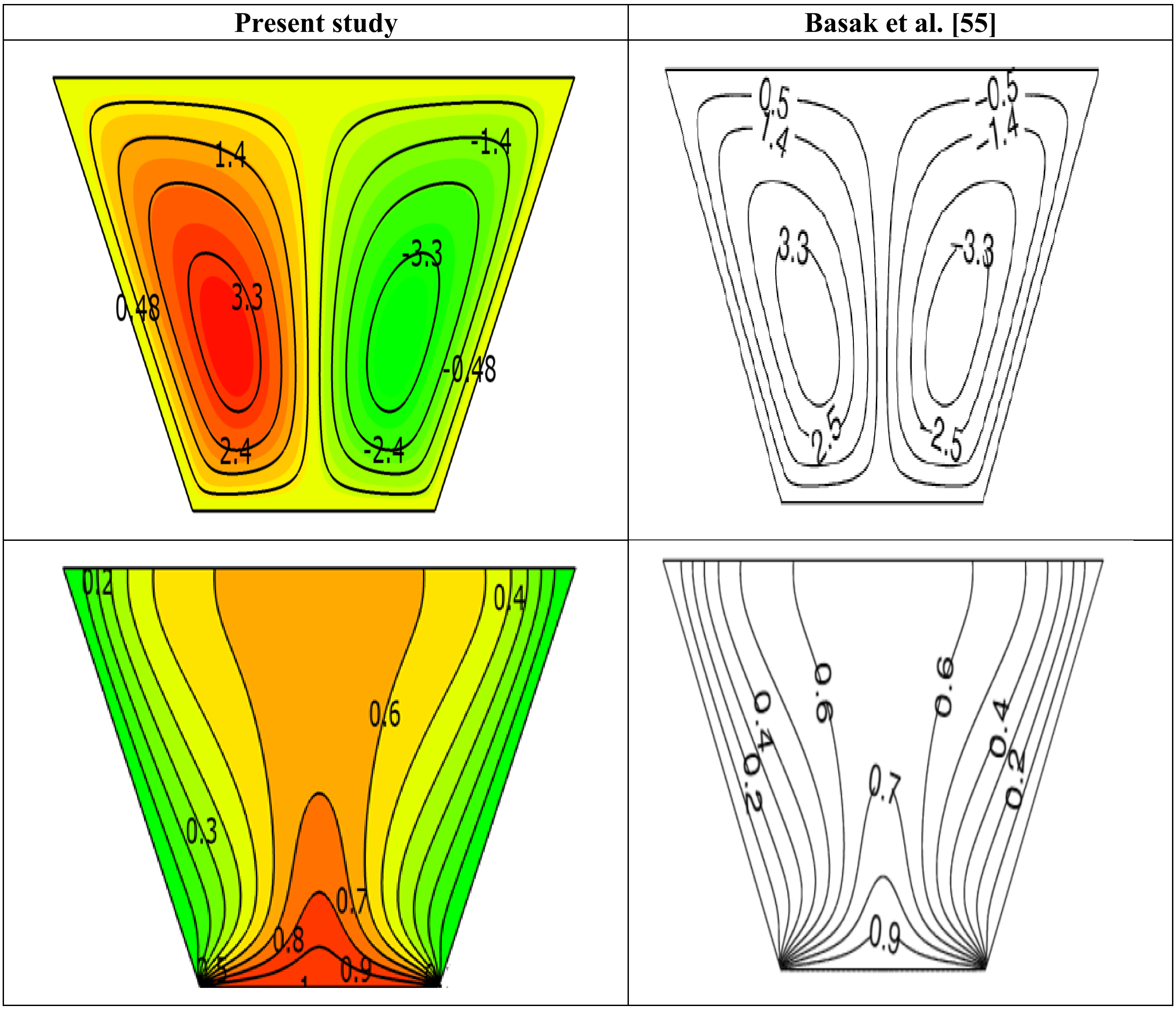

Figure 16: Stream function (top) and Isotherm (bottom) from the present study with those of Basak et al. [55].

Conclusions

Having analyzed the implications of modified Rayleigh number ($10 \leq Ra_m \leq 1000$), area ratio of the concentric trapezium $\left(\frac{1}{5} \leq AR \leq \frac{1}{3}\right)$, and Darcy number ($10^{-5} \leq Da \leq 10^{-2}$), on fluid flow and heat transfer dynamics inside the porous annulus domain created by two trapeziums, the conclusions below are made:

For Darcy number in the range of $10^{-5} \leq Da \leq 10^{-4}$, and at a modified Rayleigh number of 1000, the average heat transfer is not responsive to Darcy number increment. While for Darcy number in the range of $10^{-4} \leq Da \leq 10^{-2}$, the rate of heat transfer reduces with Darcy number increment. In the range of Rayleigh number range considered ($10 \leq Ra_m \leq 1000$), average Nusselt number improves with modified Rayleigh number increment. Also, for Darcy number in the range of $10^{-5} \leq Da \leq 10^{-4}$, and modified Rayleigh number in the range of $10 \leq Ra_m \leq 850$, average Nusselt number increases as the size of the inner trapezium increases; while for modified Rayleigh number of $850 \leq Ra_m \leq 1000$, the role of area ratio diminishes depending on the value of Darcy number (Da). For Darcy number in the range of $10^{-3} \leq Da \leq 10^{-2}$, and for the range of modified Rayleigh number considered, the average heat transfer increases as the size of the inner trapezium increases.

Data Availability Statement

The authors affirm that the data which support the results of the current investigation are present in this article.

Disclosure of Competing Interests

The authors have no conflicting interests to disclose.

References

[1] A. D. Abdulsahib, K. Al-Farhany, Review of the effects of stationary/rotating cylinder in a cavity on the convection heat transfer in porous media with/without nanofluid, Math. Model. Eng. Probl., 8(3) (2021) 356-364.

[2] I. Adegun, O. Komolafe, A. K. Hussein, J. O. (2014). A 3D finite element analysis of incompressible fluid flow and contaminant transport through a porous landfill. Int. J. Eng. Sci. Technol., *9*(4), 477-489.

[3] O. A. Olayemi, A. F. Khaled, O. J. Temitope, O. O. Victor, C. B. Odetunde, I. K. Adegun, Parametric study of natural convection heat transfer from an inclined rectangular cylinder embedded in a square enclosure, Aust. J. Mech Eng., (2021).

[4] M. Sheikholeslami, Numerical simulation of magnetic nanofluid natural convection in porous media. Phys. Lett. A, 381(5) (2017) 494-503..

[5] O. A. Olayemi, A. Salaudeen, K. Al-Farhany, R. O. Medupin, I. K. Adegun, Modelling of heat transfer characteristics around a cylindrical-barrier, Int. J. Eng. Model., 35(1) (2022) 83-106.

[6] E. Fontana, A. da Silva, F. Marcondes, Natural convection within trapezoidal enclosure with two baffles: effect of various angle of inclination, 21st Braz. Cong. Mech. (2011).

[7] A. K. Hussein, S. K. Rout, F. Fathinia, R. Chand, H. Mohammed, Technology, Natural convection in a triangular top wall enclosure with a solid strip, J. Eng. Sci., 10(10) (2015) 1326-1341.

[8] F. A. Abood, Numerical analysis of free convection in a square and in a right-angle trapezoidal enclosure filled with porous medium, Al-Qadisiyah J. Eng. Sci., 4(3) (2011) 263-273.

[9] Z. M. Al-Makhyoul, Natural convection heat transfer in trapezoidal enclosure with baffles attached to heated wall, Al-Rafidain Eng. J., 22(3) (2014)186-197.

[10] O. A. Olayemi, J. T. Olabemiwo, T. S. Jolayemi, K. O. Oladosu, C. Odetunde, I. K. Adegun, Computational fluid dynamics (CFD) analysis of buoyancy flow in a differentially heated square cavity, IOP Conf. Ser. Mater. Sci. Eng., 1107(1) (2021) 012120.

[11] A. Bejan, On the boundary layer regime in a vertical enclosure filled with a porous medium, Lett. Heat Mass Transf., 6(2)(1979) 93-102.

[12] F. Moukalled, M. Darwish, Natural convection in a partitioned trapezoidal cavity heated from the side, Numer. Heat Transf.; A: Appl. 43(5) (2003) 543-563.

[13] D. Das, M. Roy, T. Basak, Studies on natural convection within enclosures of various (non-square) shapes – A review, Int. J. Heat Mass Transf., 106(2017) 356-406.

[14] H. T. Cheong, S. Sivasankaran, Z. Siri, Effect of wall inclination on natural convection in a porous trapezoidal cavity, AIP Conf. Proc. 1605(1) (2014) 343-348.

[15] A. K. Hussein, Finite volume simulation of natural convection in a trapezoidal cavity filled with various fluids and heated from the top wall, Univers. J. Fluid Mech., 1 (2013) 24-36.

[16] I. V. Miroshnichenko, M. A. Sheremet, H. F. Oztop, K. Al-Salem, MHD natural convection in a partially open trapezoidal cavity filled with a nanofluid, Int. J. Mech. Sci., 119 (2016) 294-302.

[17] O. A. Olayemi, A. M. Obalalu, C. B. Odetunde, O. A. Ajala, Heat transfer enhancement of magnetized nanofluid flow due to a stretchable rotating disk with variable thermophysical properties effects. Eur. Phys. J. Plus, 137(3) (2022) 1-12.

[18] K. Venkatadri, O. A. Bég, P. Rajarajeswari, V. R. Prasad, Numerical simulation of thermal radiation influence on natural convection in a trapezoidal enclosure: heat flow visualization through energy flux vectors, Int. J. Mech. Sci., 171 (2020) 105391.

[19] K. Venkatadri, S. A. Gaffar, V. Prasad, B. M. H. Khan, O. A. Beg, Simulation of natural convection heat transfer in a 2-D trapezoidal enclosure, Int. J. Automot. Eng., 16(4) (2019) 7375-7390.

[20] M. Ghalambaz, M. Sabour, I. Pop, Free convection in a square cavity filled by a porous medium saturated by a nanofluid: Viscous dissipation and radiation effects, Eng. Sci. Technol. an Int. J., 19(3) (2016) 1244-1253

[21] K. L. Walker, G. M. Homsy, Convection in a porous cavity, J. Fluid Mech., 87(3) (1978) 449-474.

[22] M. A. Sheremet, T. Grosan, I. Pop, Natural convection and entropy generation in a square cavity with variable temperature side walls filled with a nanofluid: Buongiorno's mathematical model, Entropy, 19(7) (2017) 337.

[23] O. A. Olayemi, K. Al-Farhany, A. M. Obalalu, T. F. Ajide, K. R. Adebayo, Magnetoconvection around an elliptic cylinder placed in a lid-driven square enclosure subjected to internal heat generation or absorption. Heat Transfer, (2022) 1-27.

[24] M. Esfe, A. A. Abbasian Arani, W.-M. Yan, H. Ehteram, A. Aghaei, M. Afrand, Natural convection in a trapezoidal enclosure filled with carbon nanotube–EG–water nanofluid, Int. J. Heat Mass Transf., 92 (2016) 76-82.

[25] M. Hossain, M. A. Alim, L. Andallah, Numerical investigation of natural convection flow in a trapezoidal cavity with non-uniformly heated triangular block embedded inside, J. Adv. Math. Comput., 28 (2018) 1-30.

[26] R. Nikbakhti, Heat and mass transfer natural convection in a partially heated trapezoidal cavity, Int. Robot. Autom. J., 4(3) (2018) 236-240.

[27] S. Parvin, A. Akter, Analysis of natural convection flow in a trapezoidal cavity containing a rectangular heated body in presence of external oriented magnetic field, J. Sci. Res., 10(1) (2018) 11-23.

[28] A. C. Baytaş, I. Pop, Natural convection in a trapezoidal enclosure filled with a porous medium, Int. J. Eng. Sci., 39(2) (2001) 125-134.

[29] C. Beckermann, R. Viskanta, S. Ramadhyani, A numerical study of non-Darcian natural convection in a vertical enclosure filled with a porous medium, Numer. Heat Transf., 10(6) (1986) 557-570.

[30] Radhi, Z. K. , Study of natural convection in a porous trapezoidal cavity with a square body at the center of the enclosure. Eng. Techno. J., 31 (2013)(14 Part (A) Engineering).

[31] S. W. Lam, R. Gani, J. G. Symons, Experimental and numerical studies of natural convection in trapezoidal cavities. J. Heat Transf., 111(2) (1989) 372-377

[32] S. K. Saha, Numerical study of laminar natural convection heat transfer in inclined trapezoidal enclosure, J. Therm. Sci. Eng. Appl., 11(6) (2019) 061021-12.

[33] S. Sivasankaran, H. T. Cheong, M. Bhuvaneswari, Natural convection in an inclined porous triangular enclosure with various thermal boundary conditions, Therm. Sci., 23(2 Part A)(2019) 537-548.

[34] O. A. Olayemi, K. Al-Farhany, O. Olaogun, M. O. Ibiwoye, R. O. Medupin, A. Jinadu, Computational fluid dynamics analysis of mixed convection heat transfer and fluid flow in a lid-driven square cavity subjected to different heating conditions. IOP Conf. Ser. Mater. Sci. Eng., 1107(1) (2021) 012201.

[35] T. Basak, S. Roy, A. Matta, I. Pop, Analysis of heatlines for natural convection within porous trapezoidal enclosures: effect of uniform and non-uniform heating of bottom wall, Int. J. Heat Mass Transf., 53(2010) 5947-5961.

[36] T. Basak, S. Roy, A. Singh, A. R. Balakrishnan, Natural convection flows in porous trapezoidal enclosures with various inclination angles, *International Journal of Heat and* Int. J. Heat Mass Transf., 52(2009) 46127-4623.

[37] T. Adibi, R. A. Kangarluei, V. Farhangmehr, Numerical study of natural convection flow inside squared and trapezoidal cavities in various conditions. Int. J. Eng. Sci. Technol. Res. 6(5) (2017) 2278-7798.

[38] M. A. Hossain, M. Wilson, Natural convection flow in a fluid-saturated porous medium enclosed by non-isothermal walls with heat generation, Int. J. Therm. Sci., 41(5) (2002) 447-454.

[39] P. Sompong, S. Witayangkurn, Natural convection in a trapezoidal enclosure with wavy top surface, J. Appl. Math., 2013 (2013) 1-7.

[40] Y. Varol, H. F. Oztop, I. Pop, Numerical analysis of natural convection in an inclined trapezoidal enclosure filled with a porous medium, Int. J. Therm. Sci., 47(10) (2008) 1316-1331.

[41] Y. Varol, Natural convection in divided trapezoidal cavities filled with fluid saturated porous media, Int. Commun. Heat Mass Transf., 37 (2010) 1350-1358.

[42] A. Alsabery, A. Chamkha, H. Saleh, I. Hashim, B. Chanane, Darcian natural convection in an inclined trapezoidal cavity partly filled with a porous layer and partly with a nanofluid layer, Sains Malays., 46(5) (2017) 803-815.

[43] M. A. Alomari, K. Al-Farhany, A. L. Hashem, M. F. Al-Dawody, F. Redouane, O. A. Olayemi, Numerical study of mhd natural convection in trapezoidal enclosure filled with (50%mgo-50%ag/water) hybrid nanofluid: Heated sinusoidal from below, Int. J. Heat Technol., 39(4) (2021) 1271-1279.

[44] V. Kumar, A. Rani, A. K. Singh, Numerical solution of non-Darcian effects on natural convection in a rectangular inclined porous enclosure with heated walls. AIP Conf. Proc. 2177(1) (2019) 020107.

[45] F. Selimefendigil, H. F. Öztop, K. Al-Salem, Natural convection of ferrofluids in partially heated square enclosures, J. Magn. Magn. Mater., 372 (2014) 122-133.

[46] I. K. Adegun, T. S. Jolayemi, O. A. Olayemi, A. M. Adebisi, Numerical simulation of forced convective heat transfer in inclined elliptic ducts with multiple internal longitudinal fins. Alex. Eng. J., 57(4) (2018) 2485-2496.

[47] O. A., Olayemi, J. T. Olabemiwo, J. O. Dirisu, O. V. Ogunwoye, T. S. Jolayem, B. E. Anyaegbuna, T. A. Olaniyan, Numerical simulation of heat transfer and fluid flow around a cylinder of varying cross-section. Mater. Today: Proc., (2022).

[48] I. K. Adegun, S. E. Ibitoye, A. Bala, Effect of selected geometric parameters on natural convection in concentric square annulus. Aust. J. Mech. Eng., (2020)1-12.

[49] I. K. Adegun, F. L. Bello-Ochende, Mixed convective and radiative heat transfer in an inclined rotating rectangular duct with a centered circular tube. J. Braz. Soc. Mech. Sci., 26(3) (2004) 323-329.

[50] O. A. Olayemi, K. Al-Farhany, S. E. Ibitoye, A. M. Obalalu, Mixed Convective Heat Transfer in a lid-driven concentric trapezoidal enclosure: numerical simulation. Int. J. Eng. Res. Africa, 60 (2022) 43-62. Trans Tech Publications Ltd.

[51] S. E. Ahmed, A. K. Hussein, H. A. Mohammed, I. K. Adegun, X. Zhang, L. Kolsi, S. Sivasankaran, (2014). Viscous dissipation and radiation effects on MHD natural convection in a square enclosure filled with a porous medium. Nucl. Eng. Des., 266, 34-42.

[52] B. Ghasemi, S. M. Aminossadati, A. Raisi, Magnetic field effect on natural convection in a nanofluid-filled square enclosure, Int. J. Therm. Sci., 50(9) (2011) 1748-1756.

[53] S. L. Moya, E. Ramos, M. Sen, Numerical study of natural convection in a tilted rectangular porous material, Int. J. Heat Mass Transf., 30(4) (1987) 741-756.

[54] G. E. B. Malomar, C. Mbow, P. D. Tall, A. Gueye, V. B. Traore, A. C. Beye, Numerical Study of 2-D Natural Convection in a Square Porous Cavity: Effect of Three Mode Heating, Open J. Fluid Dyn., 7(1) (2017) 89-104.

[55] T.Basak, S. Roy, A. Singh, I.Pop, Finite element simulation of natural convection flow in a trapezoidal enclosure filled with porous medium due to uniform and non-uniform heating, Int. J. Heat Mass Transf., 52(2009) 70-78.